JOURNAL OF PROPULSION AND POWER
Vol. 26, No. 6, November–December 2010

Technical Notes

Wind Turbine Wall-Blockage Performance Corrections

M. J. Werle*
FloDesign Wind Turbine Corporation, Wilbraham, Massachusetts 01095

DOI: 10.2514/1.44602

Nomenclature

A	=	flow cross-sectional area
C_D	=	disc loading coefficient
C_P	=	power coefficient
C_p	=	pressure coefficient
C_T	=	propeller/blade thrust coefficient
P	=	power
p	=	pressure
u	=	nondimensional axial velocity
V	=	velocity
α	=	flow domain area ratio, i.e., blockage coefficient
ρ	=	fluid density

Subscripts

a	=	ambient freestream conditions
c	=	flow conditions for domain/conduit cross-sectional area
m	=	flow conditions for maximum power
o	=	turbine wake flow properties at downstream outlet area
p	=	conditions at the propeller plane
1,2	=	properties fore and aft of the rotor/blade, respectively

Introduction

AS DISCUSSED in [1–5], numerous studies and methodologies have been developed for estimating the influence of wall-blockage effects on either wind-tunnel or computational fluid dynamics (CFD) results, but only a limited number have addressed the cases of either a rotor or wind turbine. All such studies employ a concept introduced by Glauert [1] nearly 100 years ago for thrusting propellers and, by limited extension, for wind turbines. In that work Glauert used a momentum-balance/actuator-disc model to provide a procedure for adjusting the wind-tunnel inlet flow speed so as to generate the same thrust on the propeller in the tunnel that one would experience in an open, unencumbered condition. The resulting simple velocity adjustment relation Glauert provided has been used throughout the propulsion industry but encounters difficulty for wind turbines in which a singularity occurs for a specific thrust level. Mikkelsen and Sørensen [5] revisited the issue and, again using a momentum-balance/actuator-disc model, provided a new velocity adjustment relation that avoids Glauert's singularity. They also conducted comparisons with Navier–Stokes CFD studies that verified the predictions of the simpler momentum-balance/actuator-disc model for blockage levels of practical interest. To date, though, no method has been put forward for estimating the wall correction factors one needs to apply to measured or calculated wind turbine power levels.

The current effort extends the works of Glauert [1] and Mikkelsen and Sørensen [5]. The resulting algebraic equation set is solved numerically for a wide range of blockage levels. Additionally, exact yet simple algebraic expressions are derived for calculating the influence of wall blockage on the maximum levels of power extractable from the incoming flow; i.e., a generalized version is provided of the Betz power limit (as discussed in [6,7], for example) for unencumbered wind turbines. Finally, through use of correlation parameters suggested by the analysis, a simple approximate means is provided for directly correcting/adjusting measured and calculated power and other outputs parameter for wall-blockage effects. The utility of the resulting methodology is discussed for CFD and experimental studies of wind turbines.

Governing Equations

Following Glauert [1], Mikkelsen and Sørensen [5], and many others (see [2–4], for example), a momentum-balance/actuator-disc model of a propeller/turbine blade is employed. The control volume is as shown in Fig. 1 for which momentum, mass, and energy balances are applied to the flow structure and the cuts shown. The assumptions applied were as follows:

1) Inviscid incompressible flow is through a conduit of constant cross-sectional area A_c.

2) Flow with specified uniform pressure and velocity enters at upstream infinity.

3) Flow exits at downstream infinity at uniform pressure p_o and a slipstream occurs between the mainstream fluid exiting at velocity V_c and the fluid exiting at velocity V_o, which passed through the actuator-disc model of the rotor. The three variables p_o, V_c, and V_o are treated as unknowns.

4) The cuts around the propeller shrink to its surface.

The relevant governing equations are as follows.

Continuity:

$$A_o V_o = A_p V_p \tag{1a}$$

$$A_c V_a = A_o V_o + (A_c - A_o) V_c \tag{1b}$$

Bernoulli:

$$p_a + 1/2\rho V_a^2 = p_1 + 1/2\rho V_p^2 = p_o + 1/2\rho V_c^2 \tag{2a}$$

$$p_2 + 1/2\rho V_p^2 = p_o + 1/2\rho V_o^2 \tag{2b}$$

Momentum:

$$p_a A_c + (p_2 - p_1)A_p - p_o A_c = \rho A_o V_o^2 + \rho(A_c - A_o)V_c^2 - \rho A_c V_a^2 \tag{3}$$

Using Eqs. (1a), (1b), (2a), and (2b), the momentum equation becomes

$$(u_c - 1)(2u_o + u_c - 1) = \alpha(u_c^2 - u_o^2) \tag{4}$$

where the nondimensional velocities are defined as

$$u_o \equiv V_o/V_a, \qquad u_c \equiv V_c/V_a \tag{5a}$$

and the blockage coefficient is

Received 27 March 2009; revision received 24 May 2010; accepted for publication 24 May 2010.

*Founder and Senior Technical Advisor, 380 Main Street. Fellow AIAA.

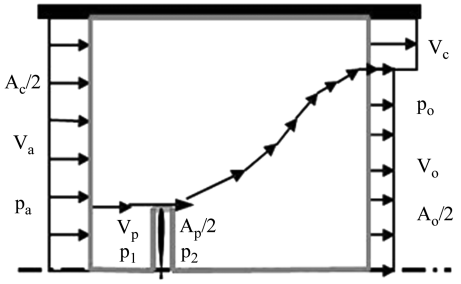

Fig. 1 Control volume.

$$\alpha \equiv A_p/A_c \tag{5b}$$

Using Eq. (4), Eq. (1b) gives the propeller velocity as

$$u_p \equiv \frac{V_p}{V_a} = u_o \frac{u_o + u_c}{2u_o + u_c - 1} \tag{6}$$

With Eq. (6) the power coefficient becomes

$$C_P \equiv P \Big/ \left(\frac{1}{2}\rho A_p V_a^3\right) = (p_1 - p_2)V_p \Big/ \left(\frac{1}{2}\rho V_a^3\right) = \frac{u_o(u_c + u_o)^2(u_c - u_o)}{2u_o + u_c - 1} \tag{7}$$

It is useful later to employ the disc loading coefficient defined as

$$C_D \equiv \frac{(p_1 - p_2)}{2\rho V_p^2} = \frac{1}{4} C_P / u_p^3 \tag{8}$$

which, with Eqs. (6) and (7), becomes

$$C_D(u_c + u_o) = (u_c - u_o)\left[1 + \frac{u_c - 1}{2u_o}\right]^2 \tag{9}$$

Two additional flow parameters of interest are as follows.
Propeller/blade thrust coefficient:

$$C_T \equiv \frac{(p_1 - p_2)}{\frac{1}{2}\rho A_p V_a^2} = u_c^2 - u_o^2 \tag{10}$$

Downstream outlet plane pressure coefficient:

$$C_{po} \equiv \frac{(p_o - p_a)}{\frac{1}{2}\rho V_a^2} = 1 - u_c^2 \tag{11}$$

For current purposes, Eqs. (4) and (9) will be taken as the governing equations for determining u_c and u_o with C_D and α as parametric variables. With this, as pointed out in [8], the solution for the limit or unencumbered case at $\alpha = 0$ can be easily recovered in closed form from Eqs. (4) and (9) as follows:
For $0 < C_D < 1$,

$$u_c = 1, \quad u_o = \frac{1 - C_D}{1 + C_D} \tag{12}$$

$$C_P = 4\frac{C_D}{(1 + C_D)^3} = \frac{1}{2} C_T[1 + \sqrt{1 - C_T}] \tag{13}$$

$$u_p = \frac{1}{(1 + C_D)} \tag{14}$$

For all $C_D > 1$,

$$u_c = 1, \qquad u_o = 0 \tag{15}$$

$$C_P = \frac{1}{2\sqrt{C_D}} = u_p, \qquad C_T = 1 \tag{16}$$

Results and Analysis

As pointed out by Mikkelsen and Sørensen [5] the above equations can be straightforwardly solved numerically. Figures 2 and 3 present

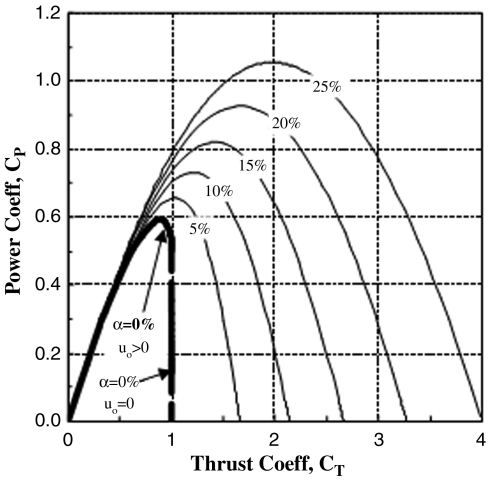

a) Power

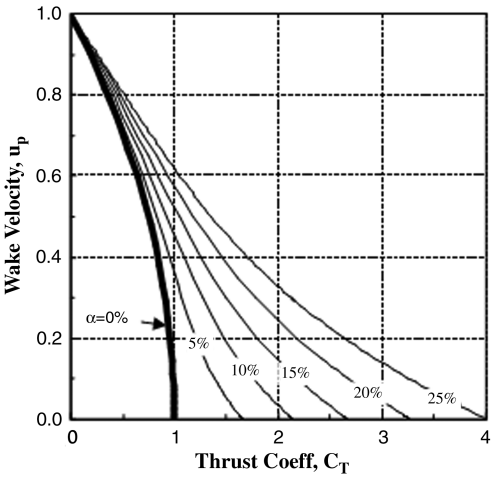

b) Wake velocity

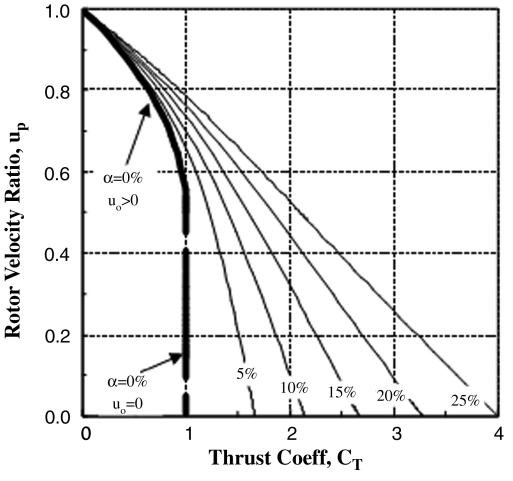

c) Rotor velocity

Fig. 2 Wall-blockage impacts on prop thrust effects.

the current solutions for values of α up to 25%. While these duplicate some of those provided by Mikkelsen and Sørensen [5], they also fill in the parameter space more thoroughly and set the stage for further useful analysis below.

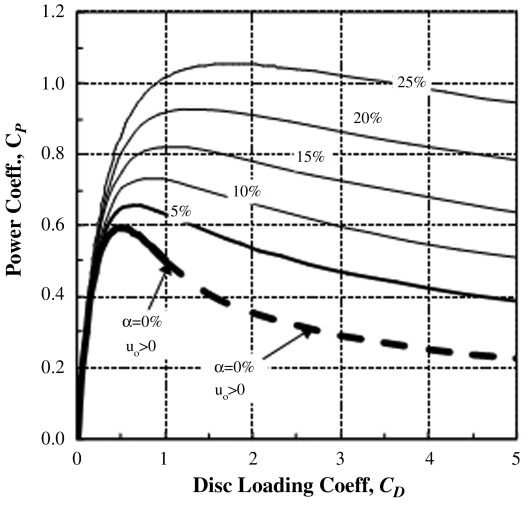

a) Power

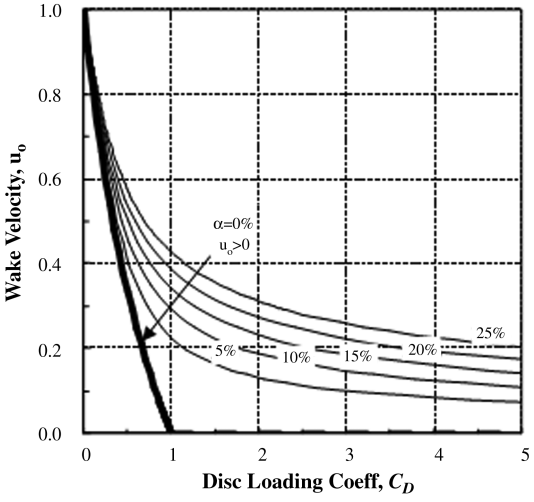

b) Wake velocity

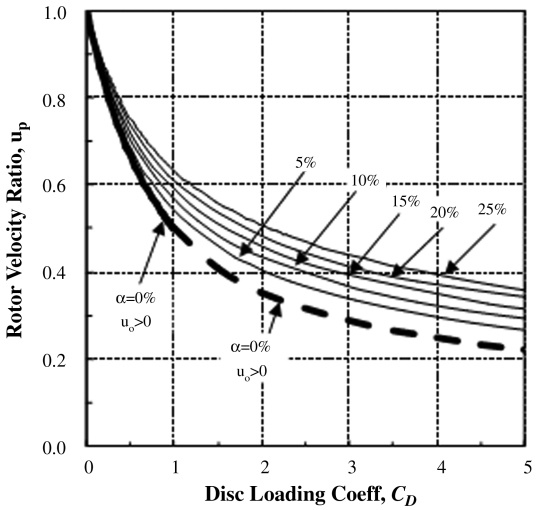

c) Rotor velocity

Fig. 3 Wall-blockage impacts on disc loading effects.

Attention is first directed to Figs. 2a–2c, where the power, wake velocities, and propeller velocities are provided, respectively. The base case of $\alpha = 0$ is highlighted for reference because it represents the sought-after state of zero wall blockage. For this case, Fig. 2a shows that C_P reaches its maximum value of 16/27 (the Betz limit) at $C_T = 8/9$. The singularity at $C_T = 1$ is apparent and involves an infinite set of C_P values between 0.5 and 0. As shown in Fig. 2b, this behavior is driven by the fact that the turbine's wake velocity at the outlet station $u_o = 0$, even though, as shown in Fig. 2c, the velocity at the propeller, $u_p < 0$. Thus, even though the system is stalled in some sense, the turbine continues to extract power.

For $\alpha > 0$, it is seen in Fig. 2a that no singularity occurs, dramatic increases in the power levels result and system stall, i.e., the $u_o = 0$ point, is seen in Fig. 2b to be delayed to much higher values of C_T. As shown in Fig. 2c, this is accompanied by a smooth drop-off in the value of the propeller velocity u_p.

The difficult aspect of employing the results provided in Fig. 2 as a basis for establishing a wall-blockage correction factor is the singularity/nonuniqueness features at $C_T = 1$ for the case of $\alpha = 0$. As shown in Fig. 3, the situation simplifies significantly when the disc loading representation is employed. Figures 3a–3c show that unique values are obtained for the power, wake velocity, and propeller velocities for all values of α and C_D. Figure 4 provides further useful information in this format. As shown in Fig. 4a, the

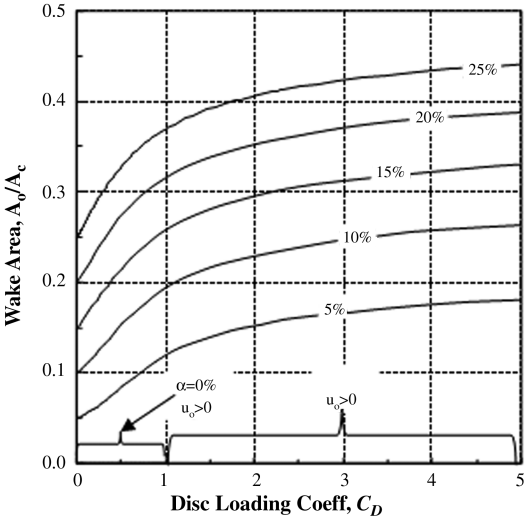

a) Wake growth

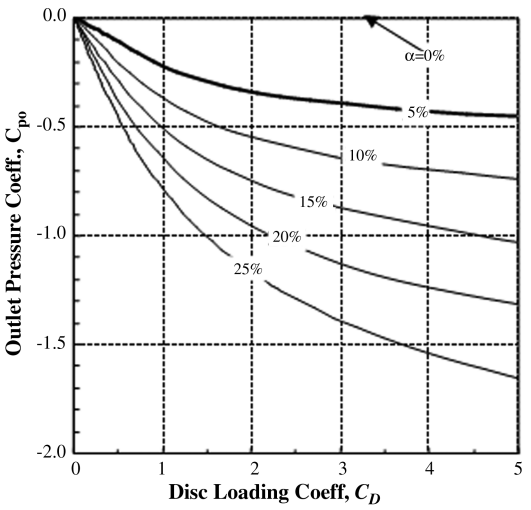

b) Outlet pressure

Fig. 4 Wall-blockage impacts on wake and pressure.

wind turbine wake area A_o/A_c is seen to grow very significantly as α increases. For example, a value of $\alpha = 25\%$ produces a wake that causes nearly 40% blockage at the outlet. This in turn causes the flow that bypasses the turbine to accelerate as manifest by the low pressure-coefficient levels shown in Fig. 4b at the outlet. The latter point gives rise to a caution that CFD methods that necessarily employ a finite domain size should avoid imposing a pressure boundary condition at the downstream outlet station.

Wall-Blockage Correction Factor

While the results presented above and by Mikkelsen and Sørensen [5] are informative, they are not useful for deriving an easily applied wall-blockage correction factor to the wind turbines' performance measures. For example, as observed in Figs. 2a and 3a, the entire power curve shifts, and it is not readily clear how one is to adjust/correct results from either a CFD or wind-tunnel study conducted at $\alpha > 0$ to the unencumbered case of $\alpha = 0$.

To that end, it is useful to first derive the parametric conditions for the maximum power condition: i.e., to establish the impact of α on maximum power extractable from the freestream. For $\alpha > 0$ this is accomplished using Eq. (7) by setting the derivative of the C_P with respect to u_o to zero and invoking Eq. (4) and its derivative to ultimately show that the maximum power at any $\alpha > 0$ occurs when

$$u_{om} \equiv (u_o)_{P=\max} = \frac{1}{3}, \qquad u_{cm} \equiv (u_c)_{P=\max} = 1 + \frac{4}{3}\frac{\alpha}{1-\alpha} \tag{17}$$

for which the maximum power extractable is determined from Eq. (7) as

$$C_{Pm} \equiv (C_P)_{P=\max} = \frac{16/27}{(1-\alpha)^2} \tag{18}$$

Additionally, with Eqs. (5), (9), and (10), one can further write that at the maximum power condition:

$$C_{Tm} \equiv (C_T)_{P=\max} = \frac{8}{9}\frac{1+\alpha}{(1-\alpha)^2} \tag{19}$$

$$C_{Dm} \equiv (C_D)_{P=\max} = \frac{1}{2}\frac{(1+\alpha)^3}{(1-\alpha)^2} \tag{20}$$

and

$$u_{pm} \equiv (u_p)_{P=\max} = \frac{2/3}{1+\alpha} \tag{21}$$

With Eqs. (18–21) one can readily calculate a correction factor for the maximum power condition (i.e., the peak points in Figs. 2 and 3), but one is left with no guidance for the remainder of the distributions. This open issue can be addressed using the correlation scheme introduced by Werle and Presz [9]. In this approach, Figs. 2a and 3a are first recast using Eqs. (18–21) to normalize both scales. As shown in Fig. 5, in comparison to Figs. 2a and 3a, this set of correlation parameters results in a near collapse of all the results to a single curve, especially for the region $C_D/C_{Dm} < 2$. For $C_D/C_{Dm} > 2$ the base case of $\alpha = 0$ is stalled and thus this region is to be avoided anyway. The near collapse of the results in Fig. 5 immediately suggests that, to a reasonable approximation, for example,

$$[C_P/C_{Pm}]_{\alpha=0} \approx [C_P/C_{Pm}]_{\alpha>0} \tag{22a}$$

which, upon use of Eq. (18), gives

$$(C_P)_{\alpha=0} \approx (1-\alpha)^2 (C_P)_{\alpha>0} \tag{22b}$$

Repeating this process for the remaining parameters leads to

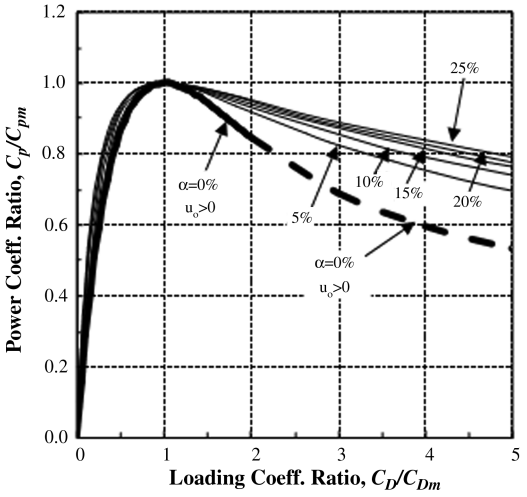

a) Disc loading impacts on power

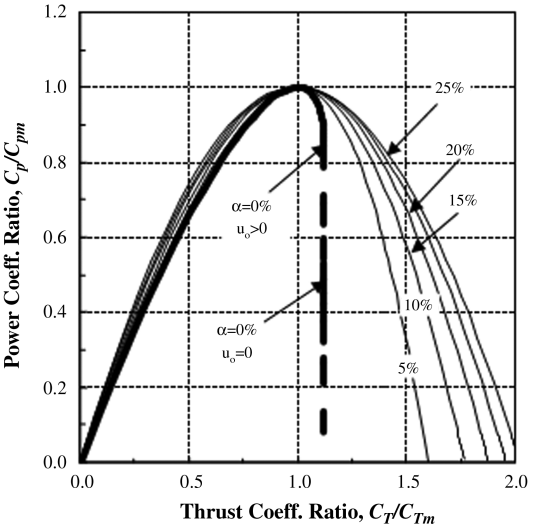

b) Thrust impacts on power

Fig. 5 Wall-blockage correlations.

$$(C_D)_{\alpha=0} \approx \frac{(1-\alpha)^2}{(1+\alpha)^3}(C_D)_{\alpha>0} \tag{23}$$

and

$$(C_T)_{\alpha=0} \approx \frac{(1-\alpha)^2}{1+\alpha}(C_T)_{\alpha>0} \tag{24}$$

Additionally one can easily show that from these, the propeller velocity correction becomes simply:

$$(u_p)_{\alpha=0} \approx (1-\alpha)(u_p)_{\alpha>0} \tag{25}$$

With Eqs. (22–25) one can adjust experimental or CFD-derived performance data obtained with $\alpha > 0$ to the unencumbered state of $\alpha = 0$. Note also that Eqs. (22–25) are exact at the maximum power condition and provide reasonable first approximations elsewhere for C_P/C_{Pm} (to within 0.1) up to $C_D/C_{Dm} = 1.5$ or $C_T/C_{Tm} = 1.25$.

Conclusions

The current results indicate and caution that large influences can be encountered for relatively small propeller-to-wind-tunnel area ratios due to the amplifying effect of the wake's downstream growth.

Further, the analysis leads to exact yet simple algebraic relations for calculating the influence of the wall-blockage effects on the

maximum power extractable from the main stream by such systems. A power-law dependency on the generalized area ratio indicates a high level of sensitivity to this parameter.

Finally, the use of a correlation schemes implied by the analysis leads to a handy approximation for quickly estimating wall-blockage corrections for either CFD or wind-tunnel studies. In turn, it also provides CFD schemes a means of achieving accurate predictions for unencumbered wind turbines using a limited-sized calculation domain with reduced number of grid points.

References

[1] Glauert, H., *The Elements of Aerofoil and Airscrew Theory*, Cambridge Univ. Press, 2nd ed., Cambridge, England, U.K., 1947.

[2] Barlow, J. B., Rae, W. H., and Pope, A., *Low-Speed Wind Tunnel Testing*, 3rd ed., Wiley, New York, 1999.

[3] Fitzgerald, R. E., "Wind Tunnel Blockage Corrections for Rotors," M.S. Thesis, Dept. of Aerospace Engineering, Univ. of Maryland, College Park MD, 2007.

[4] Loeffler, A. L., Jr., and Steinhoff, J. S., "Computation of Wind Tunnel Wall Effects in Ducted Rotor Experiments," *Journal of Aircraft*, Vol. 22, No. 3, March 1985, pp. 188–192. doi:10.2514/3.45106

[5] Mikkelsen, R., and Sørensen, J. N., "Modeling of Wind Tunnel Blockage," *Proceedings of the 2002 Global Windpower Conference and Exhibit*, European Wind Energy Association, Paris, 2002.

[6] Hansen, M. O. L., *Aerodynamics of Wind Turbines*, James & James, London, 2000.

[7] Gashe, R., and Twele, J., *Wind Power Plants*, Solarpraxis, Berlin, 2002.

[8] Werle, M. J., "Passing Through the Wind Turbine Thrust Singularity," *Journal of Propulsion and Power* (to be published); also www.flodesign.org/clients.html [retrieved 11 Aug. 2010].

[9] Werle, M. J., and Presz, W. M., Jr., "Shrouds and Ejector Augmentors for Subsonic Propulsion and Power Systems," *Journal of Propulsion and Power*, Vol. 25, No. 1, Jan.–Feb. 2009, pp. 228–236. doi:10.2514/1.36042

A. Prasad
Associate Editor